EXPERIMENTAL TECHNIQUE FOR CREEP CRACK GROWTH RATE MEASUREMENT IN A LOW CARBON STEEL

Buschiazzo A. A.
U. N. Comahue. Buenos Aires 1400, Neuquén, Argentina.
buschi@metalmat.ufrj.br

Benotti, E.
U. N. Comahue. Buenos Aires 1400, Neuquén, Argentina.

Perez Ipiña J. E.
U. N. Comahue / CONICET. Buenos Aires 1400, Neuquén, Argentina.
pipina@uncoma.edu.ar

Abstract. *The present work describes the development of techniques for measuring creep crack growth rate in metals, including the building and calibration of an electric potential drop method equipment. An old creep rupture test machine was adapted, the required devices were designed and implemented; the test method and the computations based on the ASTM E1457-98 standard test were also followed. Results from tests ranging between 1 and 170 hours on a micro-alloyed steel 1/2"T-CT specimens were analyzed and compared to those taken from literature.*

Keywords*: creep crack growth, fracture mechanics, high temperature tests.*

1. Introduction

The progressive plastic deformation of material under stress is called creep and is an important manifestation of viscoplastic behavior. Creep becomes an important design condition when service temperature exceeds 35% of the melting point of the alloy in kelvin degrees from which the component is made. The creep behaviour may be envisaged in three separated stages. The first is called primary stage in which the strain rate decreases until it reaches the minimal steady-state value of the second stage, called steady-state creep. In the third stage the creep rate begins to rise with time as necking develops until reaching rupture. In several materials, primary creep involves a short time compared to steady-state creep. The latter is more important as to design regards.

The strain rate ($\dot{\varepsilon}_{ss}$) remains constant with time in steady-state creep stage at a given stress; however, it changes significantly with stress variation, as is described by the Norton's power-law:

$$\dot{\varepsilon}_{SS} = A\sigma^n \tag{1}$$

where *A* and *n* are particular constants for each material and temperature.

The life of components with high temperature service can be estimated from creep rupture data, or from minimal strain rate data. However, these components are frequently subjected to stress or temperature gradients and it is likely that at the end of the predicted creep rupture life, a crack will develop at a high stress location and then propagate and cause failure. Failures can also result from pre-existing defects, in which case the component's entire life will be consumed by crack propagation. In these situations the traditional estimation of component's life is not proper, being very important to have the capability to predict the crack growth rate.

2. The *C*-integral*

A cracked body is assumed to be subjected to static load for sufficiently long time, so that steady-state creep has developed and engulfed the entire remaining ligament. The stress and the strain rate throughout the body are related by Eq. (1), which is analogous to the relationship between plastic strain and stress, Eq. (2), in the sub-creep temperature regime:

$$\varepsilon = \frac{\alpha\,\varepsilon_0}{\sigma_0^{\,m}}\sigma^m \tag{2}$$

where α is a constant, ε_0 and σ_0 are strain and stress, respectively, at the yield point, and *m* is the plastic exponent. Recognizing the above analogy, Landes and Begley (1976), and Nikbin, Webster and Turner (1976), independently,

defined an integral analogous to Rice's *J-Integral* (1968). Landes and Begley (1976) called this new *integral C** and defined it as follows:

$$C^* = \int_{\Gamma} W^* dy - T_i \left(\frac{\partial \dot{u}_i}{\partial x} \right) ds \tag{3}$$

where

$$W^* = \int_0^{\dot{\varepsilon}_{ij}} \sigma_{ij} \, d\dot{\varepsilon}_{ij} \ ,$$

Γ is a line contour going counterclockwise from the lower crack surface up to the upper crack surface, Fig. 1. W^* is the strain energy rate density associated with the point stress, σ_{ij}, and strain rate $\dot{\varepsilon}_{ij}$. T_i is the traction vector defined by the outward normal, n_j, along Γ. Thus, $T_i = \sigma_{ij} \, n_j$. The displacement rate vector is noted by $\dot{u}_i$, and s is the arc length along the contour.

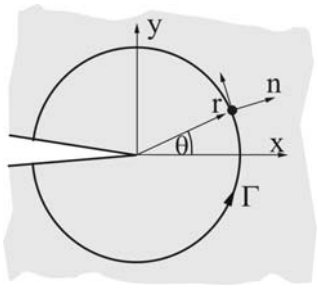

Figure 1. Crack tip coordinates.

Important consequences from this analogy are the limitations that *C*-integral* inherits from *J-Integral*. One of them is the restriction to admit crack growth. However, *C** can correlate crack growth rates if steady-state creep zone grows faster than the crack.

Materials in which the growth rate of the creep zone, $\dot{r}_C$, is higher than the creep crack growth rate, $\dot{a}$, are called creep-ductile materials. On the other hand, if $\dot{a}$ becomes comparable in magnitude to $\dot{r}_C$, they are known as creep-brittle materials. Aluminum alloys, titanium alloys, nickel base superalloys, intermetalics, and ceramics are creep-brittle materials. Some materials, depending on service conditions, may have both behaviors, as Sadananda and Shahinian (1983); and Saxena, Yagi and Tabuchi, (1994) have shown.

Based on semi-empirical methods and making use of the analogy with the *J-integral*, the following expression can be employed to approach *C**:

$$C^* = -\frac{1}{B} \int_0^{\dot{V}_{SS}} \left(\frac{\partial P}{\partial a} \right)_{\dot{V}_{SS}} d\dot{V}_{SS} \tag{4}$$

During extensive steady-state creep conditions, the following equation holds between load and $\dot{V}_{SS}$:

$$\dot{V}_{SS} = \Phi\left(\tfrac{a}{W}, n\right) P^n \tag{5}$$

As Saxena (1998) presents, combining equation (5) with (4) leads to a *C** equation for compact type C(T) specimens for $a/W > 0.4$:

$$C^*(t) = \frac{P\dot{V}_{SS}}{B_N (W-a)} \frac{n}{n+1} \left(2 + 0.522 \frac{W-a}{W} \right) \tag{6}$$

where B_N is the net thickness with side groove, $\dot{V}_{SS}$ is de steady-state load deflection rate, and n is the creep exponent, which was approximated from Nikbin´s *et al.* (2003) to n=12.5. Equation (6) is used by ASTM E1457-1998 to correlate creep crack growth rates to *C**.

The present work describes the process for updating a creep rupture test machine in order to become adequate to perform creep crack growth tests according to ASTM E1457-1998, "*Standard Test Method for Measurement of Creep Crack Growth Rates in Metals*". This involves: i) updating the temperature control, ii) carrying out the potential drop technique, iii) designing and building the extensometer device, and iv) implementating tests, estimating creep crack growth rates.

3. Method and Materials

The LPM/GMF (Laboratory of Mechanical Properties / Fracture Mechanics Group from U. N. Comahue) owns an Avery-Denison dead weight test machine, 50 kN capacity, for rupture creep test. Updating the temperature control implies a very precise and uniform control of temperature inside the furnace. The test standard states a maximum variation of ±2 ºC below 1000 ºC. Therefore, a PID control was installed, which allows to control the temperature in three independent zones of the furnace by three closed loops of control, each of them measuring temperature with a K type thermocouple.

In order to evaluate the C^* magnitude at any moment during the tests, the load line deflection must be measured. This displacement is transferred out of the furnace by means of a tube (2) and rod (5) set and two thin cantilever plates (1) and then measured by a LVDT (16), Figure 2 a).

It is important to build both the tube and the rod with the same thermally stable material to avoid wrong reading due to different thermal expansion coefficients. On the other hand, the adjustment between rod and tube has to allow an easy gliding of the rod, although avoiding misalignments which can lead to inaccurate measurements. Therefore, ceramic bushings (3 and 7 in Fig 2 a)) were used in order to take advantage from their auto-lubricating properties and then to make the axial glide of de rod easier. The materials chosen for the construction are depicted in Fig. 2 a). In order to decrease the conduction of heat flow from the furnace interior toward the LVDT, grooves on the tube external surface (5) and on the part (8) were machined. Because of the technique carried out to measure crack growth, the specimens were electrified with a current between 5 A to 40 A, depending on their sizes; then the LVDT had to be insulated by means of mica leaves, (12) and (15).

The contact between the specimen and the cantilever plates is guaranteed through two springs, (10) and (13) in Figure 2 a). As load line displacement increases during test, the two points (23) have vertical relative displacement; although they also present a horizontal component of displacement relative to the pins (24). Hence, in order to maintain both the LVDT and the extensometer parallel to the load line, part (18) guides horizontal displacement of the tube. Thus, the extensometer follows the rotation of points (23) keeping itself parallel to the load line. This guide has to be thermal an electrical insulated by means of ceramic rods (23).

The photos of Figure 2 b) and c) show the specimen and the extensometer already installed before being introduced inside the circular furnace shown on the top of the image.

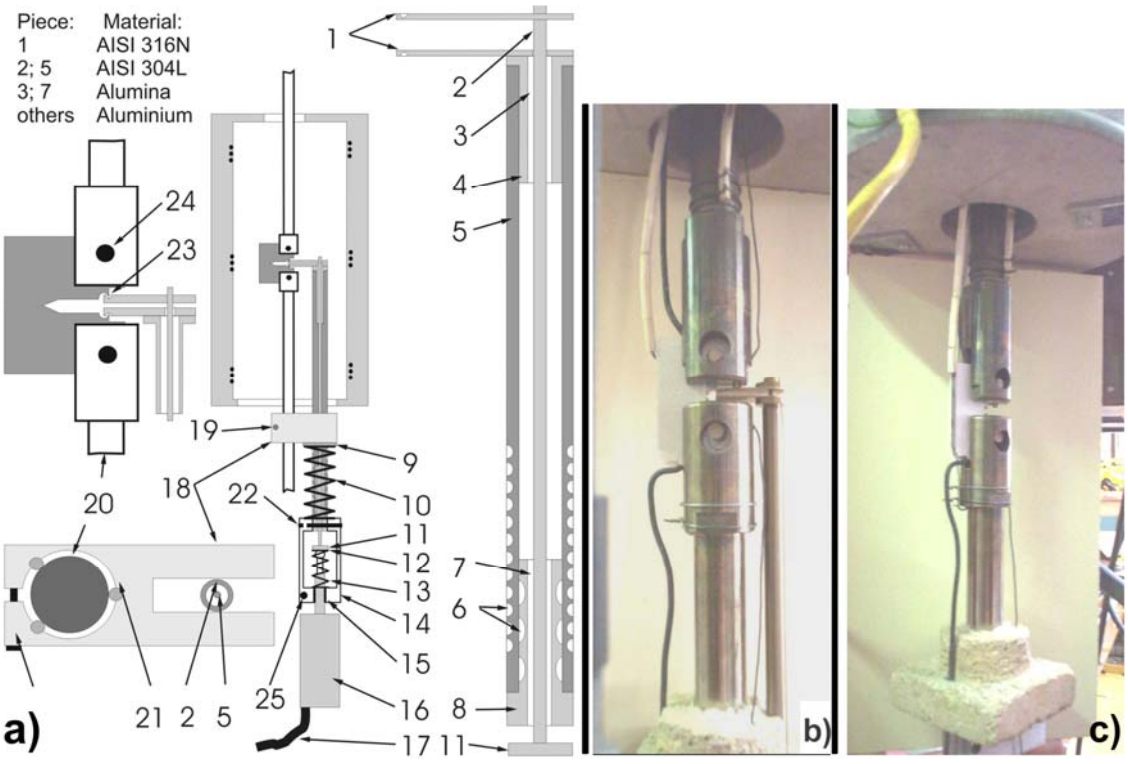

Figure 2. a) Scheme and placement of extensometer, LVDT, and accessories, b) and c) Photographies of specimen, connections, and extensometer mounted.

The clevises used were the original of the creep rupture test machine, made of Ninomic 100. It is important to note that the clevises were not totally in accordance with the test standard. Nevertheless, the available space inside the furnace inhibited from strictly following the standardized procedure. The pins used were made of Zircaloy 4, which is an alloy used in the nuclear industry. This material has good creep properties, high melting point, and its oxide is an excellent electrical insulator with good surface stability. In order to develop the insulator oxide, the pins were subjected to a heat treatment up to 400 ºC during four hours and then 600 ºC during six hours. Between the specimen and the clevises mica leaves were vertically laid, as can be noted in Figures 2 b) and c).

The material selected for testing should: i) develop extensive steady-state creep conditions in the temperature, load, and time ranges to be used, ii) present mechanical properties and creep parameters available in the literature, iii) have creep crack growth rate results already published. The material selected was an ASTM A537 class 2 steel.

Compact type specimens C(T) were used, with width W=38.1 mm (1 ½''), thickness B=5.4 mm, and separation between holes equal to 44 mm. This geometry resulted as a solution related to the free space condition in the furnace and the clevis' geometry. The specimens were fatigue pre-cracked and the tests were performed according to ASTM E1457-98 standard. The electric potential drop technique was used in order to determine the crack growth length. This technique and the making up of the associated DC current source are described in Buschiazzo *et al.* (2004).

4. Results

Some of the test features are shown in Tab. 1. Specimen 1 did not show crack growth after 66 hours test. Instead, specimen 2 experienced brittle creep behavior. Load line displacement vs. time record of specimen 3 is depicted in Figure 3, where the points of the full record and the selected points for performing the calculus in accordance with the test standard can be observed.

Table 1. Features and experimental results of tests

Specimen Nº	Type	W mm	B mm	B_N mm	a_0 mm	P kN	T ºC	I_0 A	U_0 mV	Duration hs	Δa (1) mm	Δa (2) mm
1	CT	38	5.65	-	-	5.6	360	20.5	2.25	66	0	0
2	CT	38	5.66	-	17.8	10	420	20.4	2.7	1	3.1	4.1
3	CT	38	5.44	4.95	17.5	6.5	420	20.7	2.6	169.5	5.6	6.2

(1): Average value according to the standard.
(2): Estimated value from electric potential drop technique.

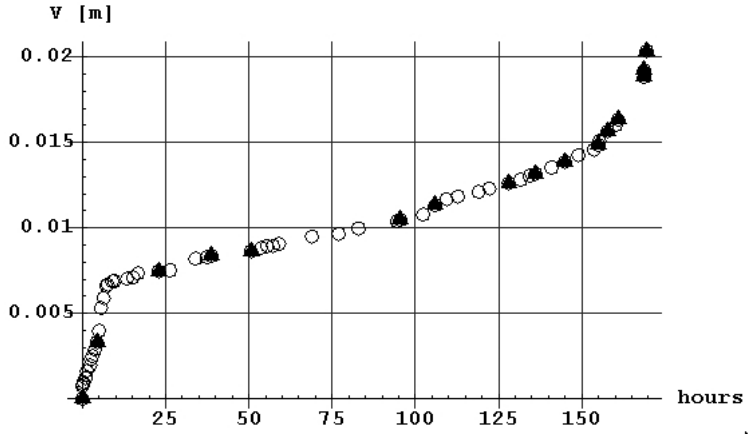

Figure 3: Load line displacement vs. time record of specimen 3.

In order to estimate the crack growth rate as function of C^* parameter, da/dt has to be calculated in the first place. Afterwards, C* has to be calculated in each selected point, the load line displacement rate component due to creep having to be known. Figure 4 presents the crack growth rate obtained in this way.

According to the validity criteria in the standard, various points are not valid for which $\dot{V}_C / \dot{V} \leq 0{,}5$. Figure 5 shows that all the acquired points for specimen 2 are invalid, meaning that this material showed a brittle-to-creep behavior for the load and temperature tested.

Figure 6 shows the correlation between crack growth rate and C^*. The closed points are the valid ones according to the validity criteria. As standard indicates, the transition time, t_T, after which C* characterizes crack growth rate, was

between 50.6 and 95.4 hours. The $\dot{V}_C/\dot{V}$ ratio was larger than 0.5 up to 157.9 hours of testing, as shown in Fig. 5. In this way, points corresponding to times between 95 and 158 hours, approximately, are considered valid.

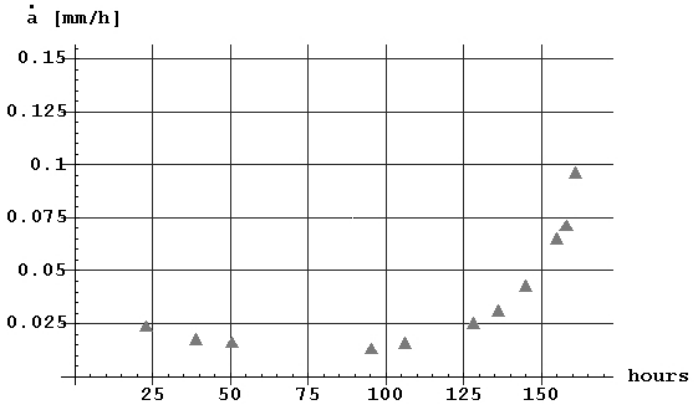

Figure 4. Crack growth of specimen 3.

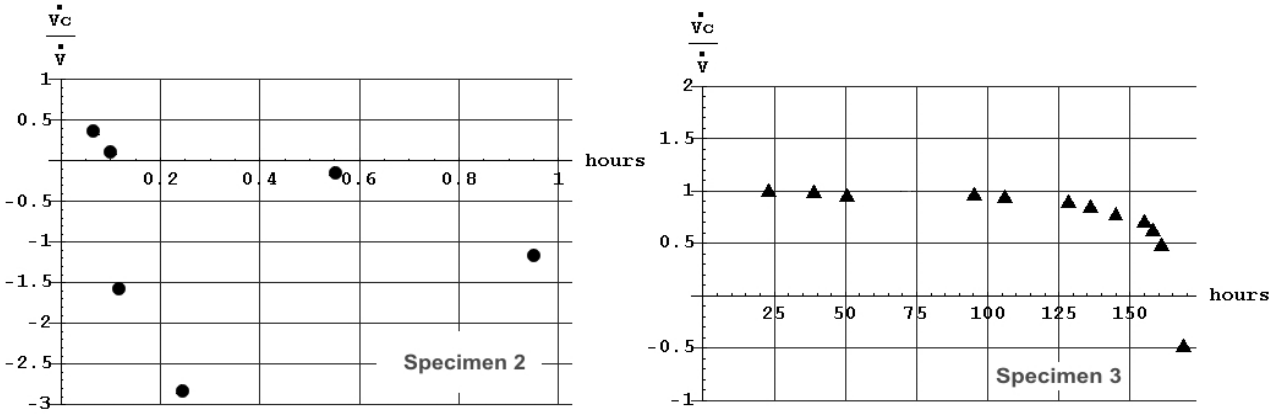

Figure 5. $\dot{V}_C/\dot{V}$ ratio for specimens 2 and 3.

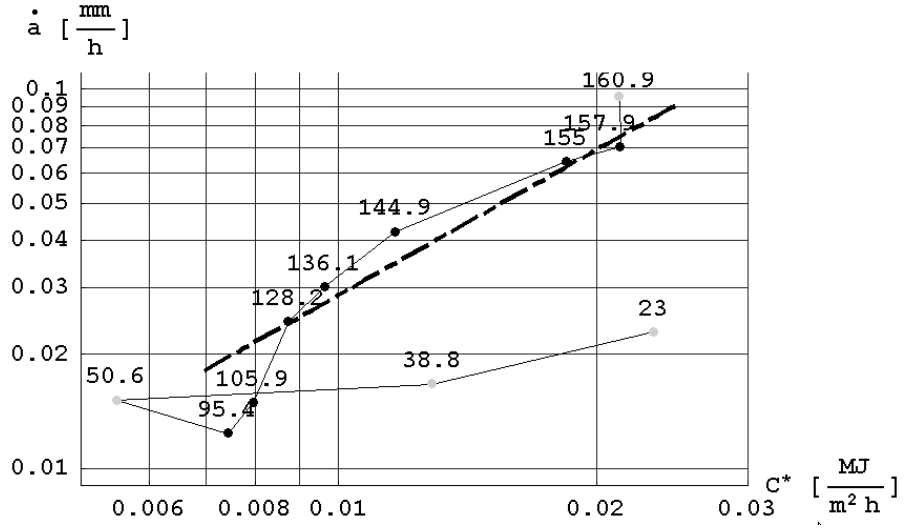

Figure 6. Creep crack growth rate vs. C* parameter of specimen 3.

The crack growth rate is often expressed according to the following expression:

$$\dot{a} = A\left(C^*\right)^q \tag{7}$$

where A and q are material constants. Figure 6 also shows the curve that resulted from fitting by square minimum difference the valid points, resulting A=9.94 and q=1.27.

5. Discussion

The three thermocouples reported temperatures differing no more than ±1 ºC, being ±2 ºC the maximum deviation allowed by the standard for the test temperature. The furnace division into three independent sectors proved effective.

The displacement measurement device, that was developed and implemented for these tests, generated load line displacement, *V,* vs. time curves similar to and in accordance with those found in the bibliography, Saxena, Yagi, and Tabuchi (1994). No more precise calibrations were made in order to verify the actual *V*. This device did not present any inconvenient during the *V* measurements and their characteristics as electric and thermal insulating proved satisfactory.

The pins made of Zircaloy 4 worked properly transferring the load and also electrically insulating the specimen. Although the compact specimen geometry did not have the proportions suggested by the standard, alterations in the J calculations in literature were not proposed.

The current source, working at an intensity of 20 A, showed reliable in tests lasting up to 170 hours. A small scatter in the potential drop values was appreciated and was attributed to variations in the line voltage, generated by the start up and end down of high consuming equipment inside the laboratory, as air conditioning system and other electrical engines. It must be reminded that the current source developed for the present work was devised in order to maintain a constant current for any charge variation, although it was not designed to maintain the current intensity whenever the line voltage varies. In order to diminish this scatter, the use of a voltage stabilizer is suggested. A closed loop to eliminate the effects of perturbations in the line voltage will be implemented in the near future.

In spite of that scatter, the stable crack growth due to creep was characterized satisfactorily, thanks to the filtering tools that the standard proposes in point 10.3.1. The potential drop technique gave a crack growth prediction corresponding to specimen 3, 170 hours, which was completely correct. The prediction of null crack growth in specimen 1 was also correct.

As to the diminishing in potential drop near the test beginning, similar results are found in literature. This effect is attributed by Wilkowski and Maxey (1993), to the crack tip blunting.

There is an important aspect to be discussed - the test corresponding to specimen 2, which was an invalid one. This specimen had no side grooving and suffered important lateral contraction, meaning a reduction in the remaining ligament on the virtual crack plane. In terms of currents, this means an increment of resistance that is interpreted as a crack growth by the calculations related to the technique, overestimating then the crack growth in values over the 15% admitted by the standard. Consistently with this analysis, the crack growth in specimen 3 was correct because the side grooving prevented lateral contraction.

A perturbation in the small electrical signal was found, and it was proved that it was originated during the start up and end down of the power cycles in the electrical resistances of the furnace. Then, during the short periods where the potential drop was measured, the temperature control was turned off.

For load line displacement rate calculation, $\dot{V}_C$, material's constants were estimated (particularly m and $D1$ from Ramberg-Osgood expression, item 10.4 in the standard) from the paper by Fookes and Smith (2003), who made tests at lower temperature (380 ºC) although using a similar material. These constants were underestimated and gave higher $\dot{V}_c$ values, and then higher C^* in the present tests, performed at 420 ºC. Mathematically, and as a first approximation, the former analysis explains that the results corresponding to specimen 3 were displaced to the right in Fig. 7.

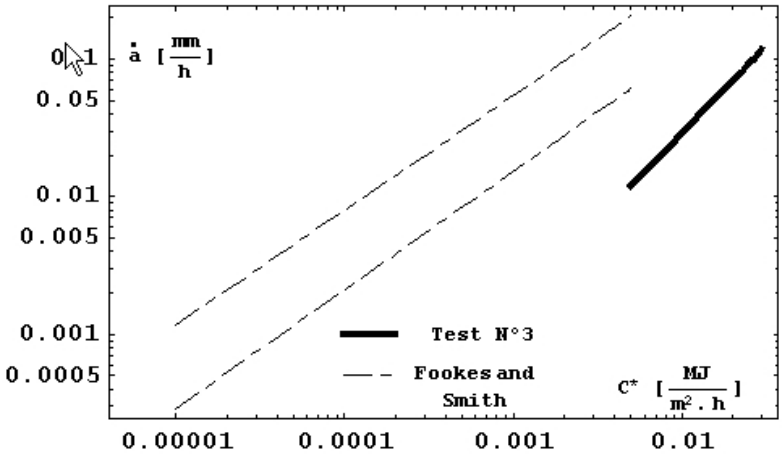

Figure 7. Comparison of results.

The test standard establishes that only for those points where $\dot{V}_c / \dot{V} > 0{,}5$, their crack growth rates can be correlated to *C**. Data falling out of this condition are considered invalid (brittle creep behavior). The total displacement rate, $\dot{V}$, can be decomposed into two components; one caused by *creep*, $\dot{V}_c$, and the other elastic component due to crack growth, $\dot{V}_e$. Negative $\dot{V}_c$ values, as those in specimen 2, mean that the elastic component is larger than that due to creep. From this last statement, it can be guessed that the crack is growing at a larger velocity than the region ahead the crack tip subjected to creep. The former condition was not satisfied at any point in specimen 2, having presented also negative values. This suggests that another creep crack growth parameter, as the stress intensity factor or the J-integral, can be used, as Gill, Saxena, and Bloom (1994) indicate.

For the case of specimen 3, from all conditions imposed by the standard, only that establishing $V < 0{,}05W$ was not fulfilled. This test showed a ductile to creep behavior, being then characterizable by the parameter *C**.

6. Conclusion

The electric furnace performance was modified, with excellent results, to fulfill the standard requirements.

The work conditions of the extensometer were complicated because of restricted space, suitable strength and fit of its parts, added to electrical and thermal isolation requirements; nevertheless, the extensometer presented an adequate design and performed its function properly.

Pins made of Zircaloy 4 were implemented as devices to transfer the testing load to specimen, holding the electrical and thermal isolation properties necessary for these tests.

The electric potential drop technique showed adequate results and can be improved by incorporating a stabilized tension source. In addition, side grooving must be performed when significant lateral contraction could exist.

In order to calculate the fracture parameter *C*,* material properties were estimated based on bibliography data of tests performed at lower temperature. Results were compared and disagreements were mathematically interpreted.

Brittle and ductile creep behaviors, depending on the applied load, were experienced by the same material.

7. Acknowledgements

To Roberto Haddad, CAC CNEA, and Jorge Bergaglio, CAB CNEA for the technical support.

8. References

ASTM E1457-98, 1998, *"Standard Test Method for Measurement of Creep Crack Growth Rates in Metals*". Published in May.

Buschiazzo A. A., Visentin M. Saavedra H. y Perez Ipiña J. E., 2004, "Método de Caída de Potencial para Medición de Crecimiento de Fisura". Cuaderno de Facultad Nº 007/2004, F. I. U. N. Comahue.

Fookes A. J *and* D. J. Smith, 2003, "*The influence of plasticity in creep crack growth in steels*". *Int J Pressure Vessels & Piping* 80, 453-463.

Gill Y., Saxena A. *and* J. M. Bloom, 1994, "*Creep Crack Growth Behavior of a SA-106C Carbon Steel*", *unpublished research, Georgia Institute of Technology, Atlanta, Georgia*.

Landes J. D. *and* Begley J. A., 1976, "*A Fracture Mechanics Approach to Creep Crack Growth*"*ASTM STP 950,* pp. 128-148.

Nikbin K. M., Webster G. A., *and* Turner C. E., 1976, " *Relevance of Nonlinear Fracture Mechanics to Creep Crack Growth*", *ASTM STP 601,* pp.47-62.

Nikbin K. M., Yatomi M., Wasmer K. *and* Wester G. A., 2003, *"Probabilistic analysis of creep crack initiation and growth in pipe components*", *Int J Pressure Vessels & Piping* 80, 585-595.

Rice J.R, 1968 "*A Path Independent Integral and The Aproximate Analysis of Strain Concentration by Notches and Cracks*". J. Appld Mech., 55(E2), pp.379-386.

Sadananda K *and*, Shahinian P., 1983, "*Evaluation of J*-Parameter for Creep Crack Growth in Type 316 Stainless Steel*", *ASTM STP 791,* pp II-182-II196.

Saxena A., 1998 "*Nonlinear Fracture Mechanics for Engineers*". CRC Press LLC.

Saxena, A., Yagi, K. *and* Tabuchi, M., 1994, "*Crack Growth Small Scale and Transition Creep Conditions in Creep-Ductile Materials", ASTM STP 1207,* pp.481-497.

Wilkowski, G. M. *and* Maxey, W. A., 1993, "*Review and Applications of the Electrical Potencial Method for Measuring Crack Growth in Specimens, Flawed Pipes, and Pressure Vessels*", ASTM STP 791, pp II-266-II-294.

9. Responsibility notice

The authors Buschiazzo A. A., Perez Ipiña J. E. and Benotti E. are the only responsible for the printed material included in this paper.